

## Supporting information

### **Synergistic effect of mesoporous Mn<sub>2</sub>O<sub>3</sub>-supported Pd nanoparticle catalysts for electrocatalytic oxygen reduction reaction with enhanced performance in alkaline medium**

**Hui-Qing Dong, Yu-Yun, Chen, Min Han, Ji-Sen Li, Jie Zhang, Ji-Sen Li, Ya-Qian Lan,\* Zhi-Hui Dai and Jian-Chun Bao\***

Jiangsu Key Laboratory of Biomedical Materials, College of Chemistry and Materials Science,  
Nanjing Normal University, Nanjing 210023, People's Republic of China,  
E-mail: [yqlan@njnu.edu.cn](mailto:yqlan@njnu.edu.cn); [baojianchun@njnu.edu.cn](mailto:baojianchun@njnu.edu.cn);

## **I. Experimental Section**

### **1. Materials Synthesis**

#### **Synthesis of meoporous Mn<sub>2</sub>O<sub>3</sub> nanostructure**

In a typical synthesis, 0.519 g Mn(CH<sub>3</sub>COO)<sub>2</sub> and 0.1224 g sodium dodecyl sulfate (SDS) were dissolved in 50 mL deionized water with magnetic stirring. After stirring for 30 min, 50 mL deionized water containing 0.328 g Na<sub>3</sub>PO<sub>4</sub> and 0.1224 g SDS were added into above solution with stirring, white precipitation appeared immediately in the mixed solution. Then tetrabutyl ammonium hydroxide aqueous solution (10%) was employed to adjust the pH value of the reaction solution to 9-10, this range is favor of Mn<sup>3+</sup> exist. During this process, the colour of the precipitation was from white to brick-red and become brown ultimately. The above mixture was kept at 80 °C in oil bath with magnetic stirring to ensure a complete reaction for 3 hours. The obtained homogeneous brown precipitate was washed several times by deionized water and ethanol, and dried in vacuum oven at 40 °C overnight.

#### **Synthesis of mesoporous Pd-Mn<sub>2</sub>O<sub>3</sub> nanocomposites**

A certain amount of Mn<sub>2</sub>O<sub>3</sub> was mixed 10 mL of absolute ethanol in a 15 mL Teflon container, then 0.0266 g of Pd(NO<sub>3</sub>)<sub>2</sub> was added to the above reactor. The mixture was stirred for 1 hour and subsequently held at 130 °C for 8 hours. After the reaction, the obtained dark precipitate was separated by filtration, and followed by washing with deionized water and ethanol under ultrasonic irradiation and dried in vacuum oven at 40 °C overnight.

### **2. Materials Characterization**

The transmission electron microscopy (TEM) images were taken on a JEM-200CX instrument (Japan), using an accelerating voltage of 200 kV. High-Resolution transmission electron microscopy (HRTEM) images were obtained on JEOL-2100F apparatus at an accelerating voltage of 200 kV. The X-Ray energy dispersive spectra (EDS) were taken on a JSM-5610LV-Vantage typed energy spectrometer. The powder X-Ray diffraction (XRD) patterns were recorded on a D/max 2500VL/PC diffractometer (Japan) equipped with graphite monochromatized Cu K $\alpha$  radiation ( $\lambda =$

1.54060 Å). Corresponding work voltage and current is 40 kV and 100 mA, respectively. Search-Mach software was used to deal with the acquired diffraction data. The X-ray photoelectron spectroscopy (XPS) measurements were carried out on a PHI 5000 Versa Probe (Japan) photoelectron spectrometer using a monochromatic Al K $\alpha$  X-ray source. The Brunauer-Emmett-Teller (BET) specific surface areas were determined from nitrogen adsorption desorption isotherms that were carried out on a ASAP 2050 static volumetric absorption analyzer (American). Actual Pd loadings of the Pd-Mn<sub>2</sub>O<sub>3</sub> nanocomposites were determined by the inductively coupled plasma atomic emission spectroscopy (ICP-AES) technique using an IRTS INTREPID II XSP (Thermo Electron CORPORATION, USA) instrument.

### 3. Electrode Preparation and Electrochemical Test

Rotational disk electrode (RDE) with glassy carbon (GC) substrate was used to confine the catalyst for measurements. Prior to use, the GC electrode was polished with alumina slurry and then cleaned ultrasonically with ethanol and distilled water. The catalyst-modified electrode was prepared as follows. 4 mg of the obtained catalysts were dispersed into 2 mL 5:1 v/v water/ethanol mixed solvent and obtained a suspension. The concentration of the suspension was about 2 mg/mL. Then the resultant suspension was ultrasonicated for at least 30 min to generate a homogeneous ink. Next, 10  $\mu$ L of the dispersion was dropcast onto the GCs, leading to the catalysts loading  $\sim 1\text{mg}/\text{cm}^2$ . After the GCs was dried at room temperature for 10min, 5  $\mu$ L (1wt%) of Nafion solution was dropped on the electrode surface and dried at room temperature. For comparison, the pure mesoporous Mn<sub>2</sub>O<sub>3</sub> nanostructure modified was also dried for electrochemical measurement.

The electrocatalytic performances of various modified GCs were tested in electrochemical cell with a three-electrode configuration. A Pt wire and a saturated calomel electrode (SCE) were used as an auxiliary and reference electrodes, respectively. The above described RDE coated with catalyst was applied as the working electrode. Rotating disk voltammetry was performed on Gamry's Rotating Disk Electrode (RDE710) at a rotating rate of 1600 rpm. O<sub>2</sub> reduction reactions were examined by first bubbling the electrolyte solution (0.1 M KOH) with high purity O<sub>2</sub>

for 20 min and then keeping the solution with an O<sub>2</sub> atmosphere during the entire experimental procedure. All electrochemical experiments were carried out with a CHI 700E electrochemistry workstation (Shanghai Chenhua Instrument Factory China) at room temperature.

The overall electron transfer number per oxygen molecule involved in the typical ORR process can be calculated from the slopes of the Koutecky-Levich plots using the following equation:<sup>1</sup>

$$\frac{1}{J} = \frac{1}{J_L} + \frac{1}{J_K} = \frac{1}{B\omega^{1/2}} + \frac{1}{J_K}$$
$$B = 0.62nAFC_0D_0^{2/3}\nu^{-1/6}; J_K = nFAkC_0$$

in which  $J$  is the measured current density,  $J_K$  and  $J_L$  are the kinetic and diffusion-limiting current densities,  $\omega$  is the angular velocity of disk ( $\omega=2\pi N$ ,  $N$  is the rotation speed),  $n$  is the overall number of electrons transferred in the ORR,  $F$  is the Faraday constant ( $F=96485 \text{ C}\cdot\text{mol}^{-1}$ ),  $A$  is the geometric electrode area ( $\text{cm}^2$ ),  $C^0$  is the saturated O<sub>2</sub> concentration in the electrolyte,  $D^0$  is the diffusion coefficient of O<sub>2</sub>,  $\nu$  is the kinematic viscosity of electrolyte, and  $k$  is the electron-transfer rate constant.

#### References:

1. W. S. Hummers and R. E. Offeman, *J. Am. Chem. Soc.*, 1958, **80**, 1339.

## II. Supplementary Figures

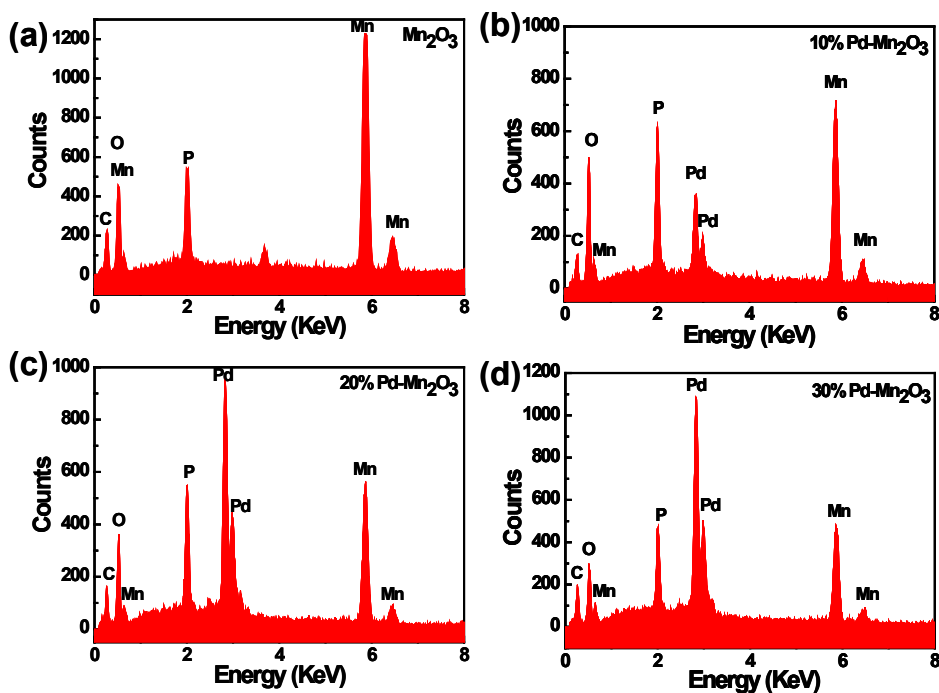


Fig. S1 EDS spectra for (a) mesoporous  $\text{Mn}_2\text{O}_3$  nanostructure, (b) 10% Pd- $\text{Mn}_2\text{O}_3$  nanocomposites, (c) 20% Pd- $\text{Mn}_2\text{O}_3$  nanocomposites and (d) 30% Pd- $\text{Mn}_2\text{O}_3$  nanocomposites, respectively.

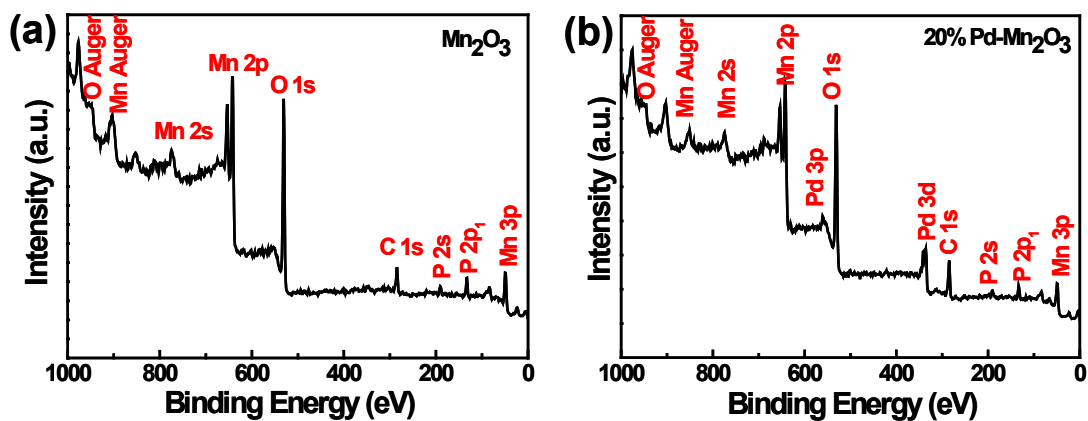
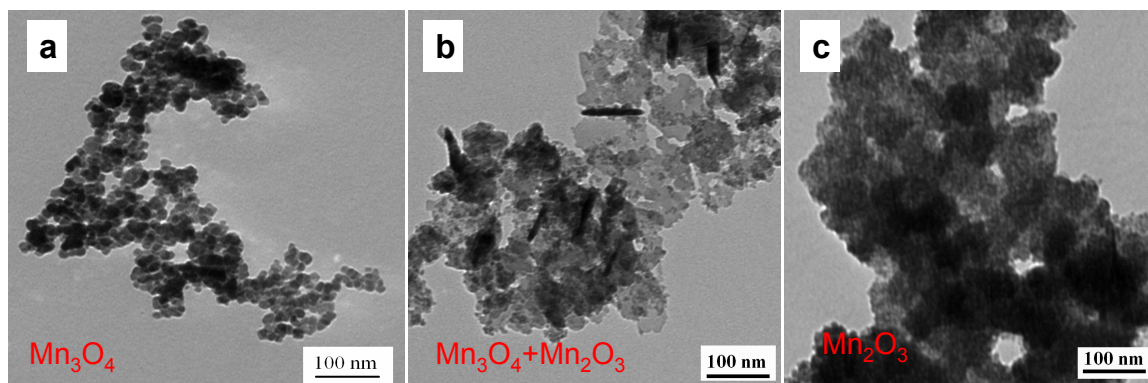
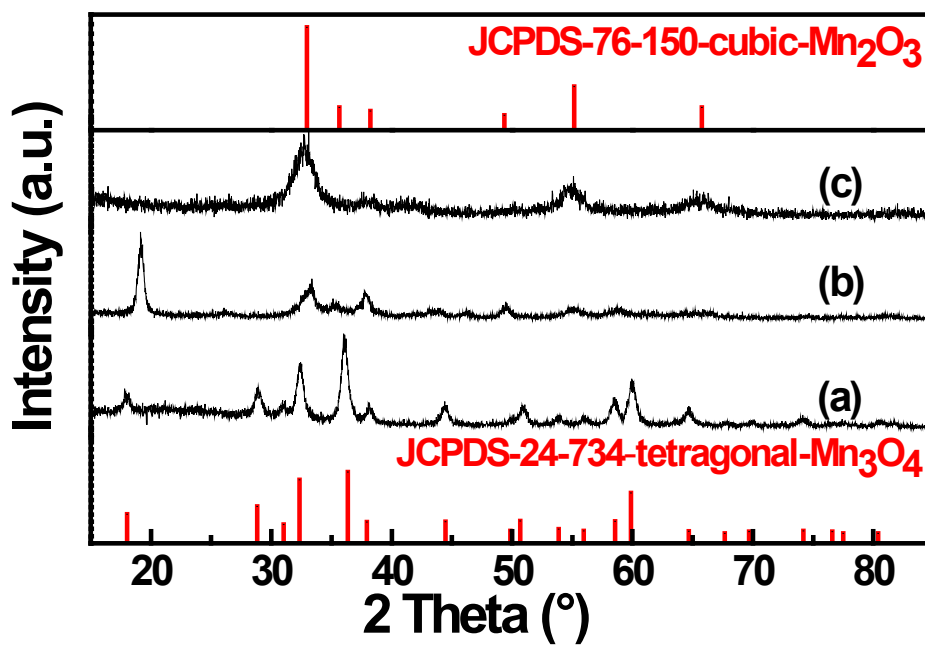


Fig. S2 XPS spectra of (a)  $\text{Mn}_2\text{O}_3$  nanostructure and (b) 20% Pd- $\text{Mn}_2\text{O}_3$  nanocomposites.



**Fig. S3** TEM images of the obtained samples with different dosage of  $\text{Na}_3\text{PO}_4$ , (a) 0 g, (b) 0.164 g and (c) 0.328 g, respectively.



**Fig. S4** XRD patterns of obtained samples with different dosage of  $\text{Na}_3\text{PO}_4$ , (a) 0 g, (b) 0.164 g and (c) 0.328 g, respectively.

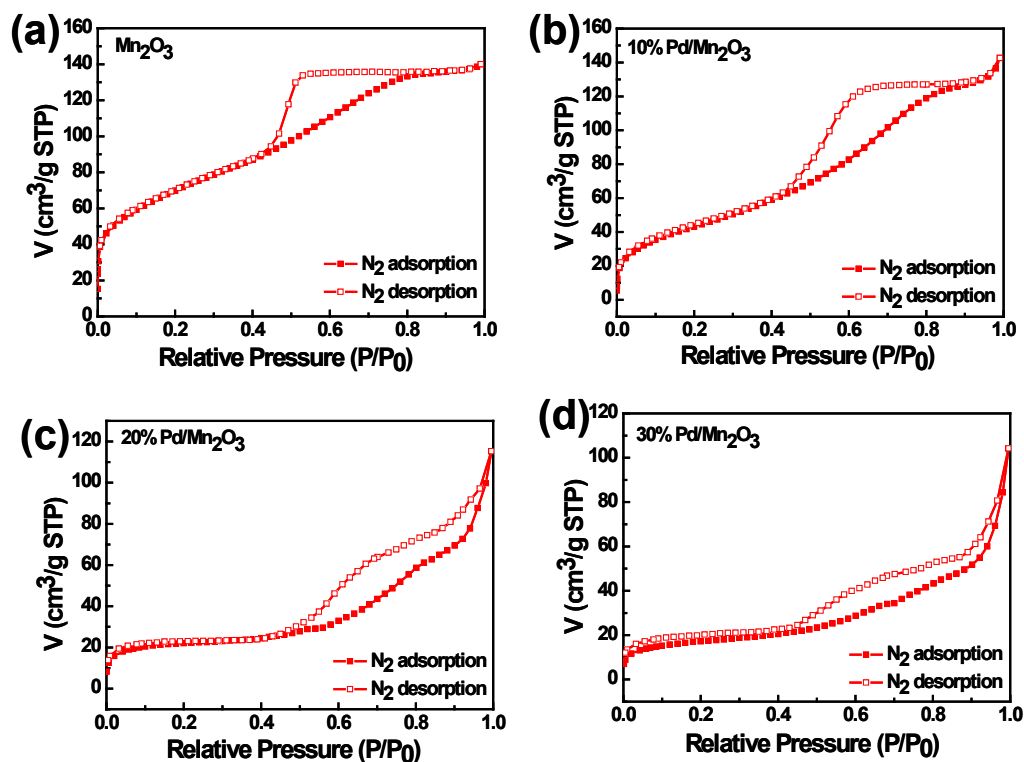


**Fig. S5** N<sub>2</sub> adsorption-desorption isotherms of (a) mesoporous Mn<sub>2</sub>O<sub>3</sub> nanostructure, (b) 10% Pd-Mn<sub>2</sub>O<sub>3</sub> nanocomposites, (c) 20% Pd-Mn<sub>2</sub>O<sub>3</sub> nanocomposites and (d) 30% Pd-Mn<sub>2</sub>O<sub>3</sub> nanocomposites, respectively.

**Table S1** The BET surface area and pore size data of Mn<sub>2</sub>O<sub>3</sub> and Pd-Mn<sub>2</sub>O<sub>3</sub> nanocomposites.

sample	Mn <sub>2</sub> O <sub>3</sub>	10% Pd-Mn <sub>2</sub> O <sub>3</sub>	20% Pd-Mn <sub>2</sub> O <sub>3</sub>	30% Pd-Mn <sub>2</sub> O <sub>3</sub>
BET surface area (m <sup>2</sup> ·g <sup>-1</sup> )	246.6103	159.8959	70.2298	57.8024
Pore width (nm)	3.7	4.2	4.4	4.2

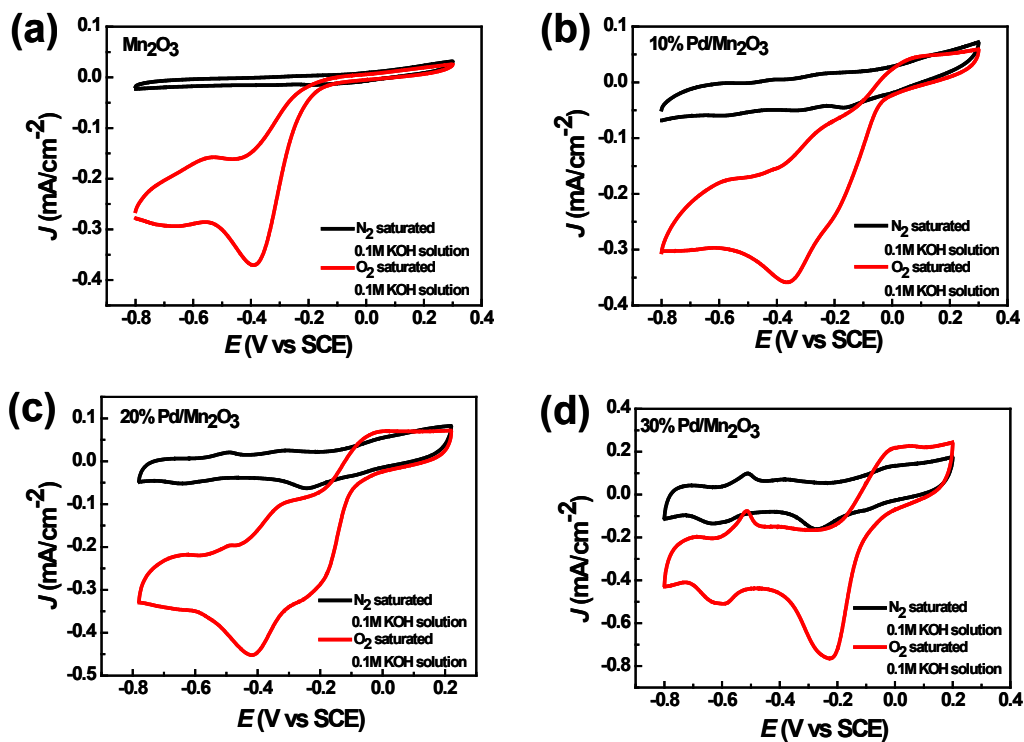


Fig. S6 Cyclic Voltammograms for (a) mesoporous  $Mn_2O_3$  nanostructure, (b) 10% Pd- $Mn_2O_3$  nanocomposites, (c) 20% Pd- $Mn_2O_3$  nanocomposites and (d) 30% Pd- $Mn_2O_3$  nanocomposites, respectively.

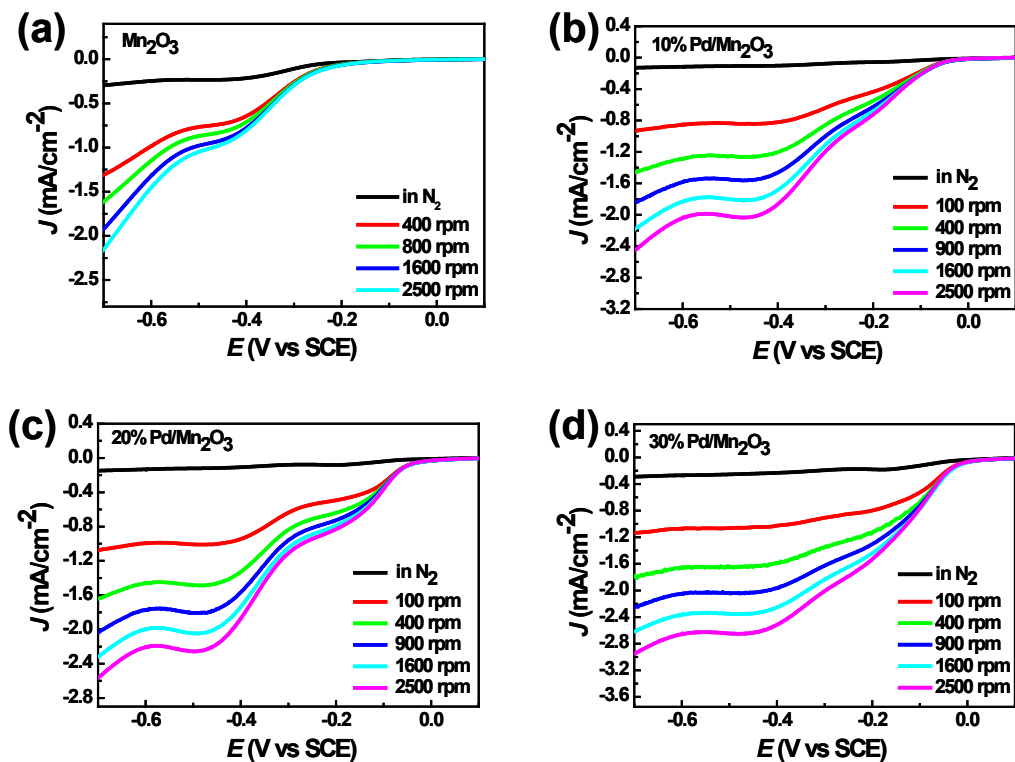
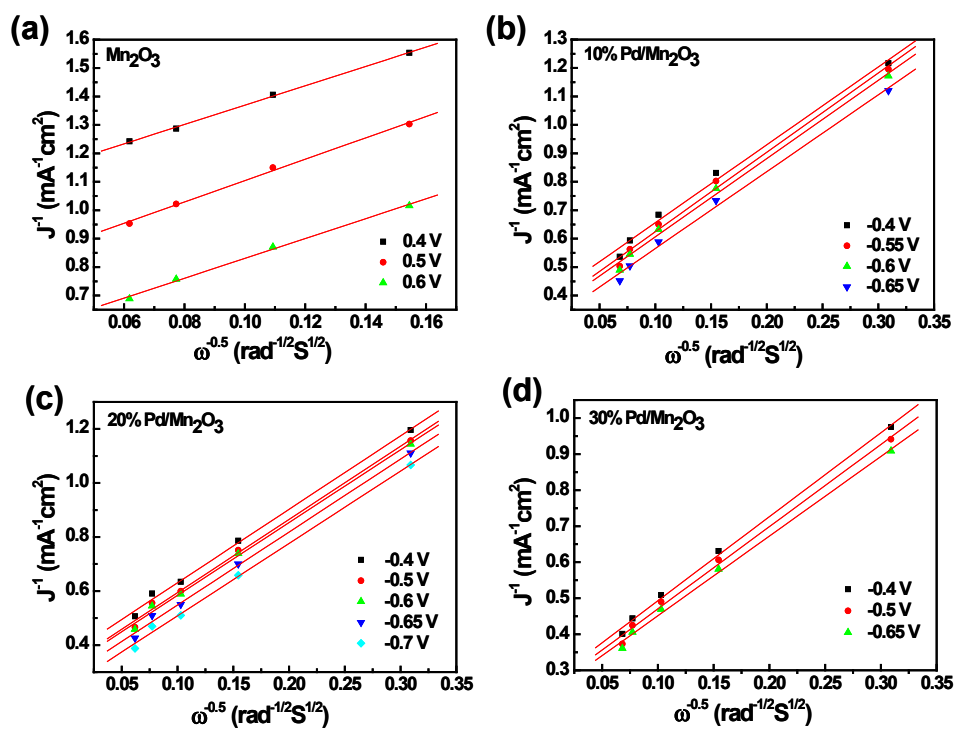


Fig. S7 Linear scanning voltammograms for (a) mesoporous  $Mn_2O_3$  nanostructure, (b) 10% Pd- $Mn_2O_3$  nanocomposites, (c) 20% Pd- $Mn_2O_3$  nanocomposites and (d) 30% Pd- $Mn_2O_3$  nanocomposites, respectively.



nanocomposites, respectively at different rotating rates.



**Fig. S8** Koutecky-Levich Plots for (a) mesoporous Mn<sub>2</sub>O<sub>3</sub> nanostructures, (b) 10% Pd-Mn<sub>2</sub>O<sub>3</sub> nanocomposites, (c) 20% Pd-Mn<sub>2</sub>O<sub>3</sub> nanocomposites and (d) 30% Pd-Mn<sub>2</sub>O<sub>3</sub> nanocomposites, respectively.

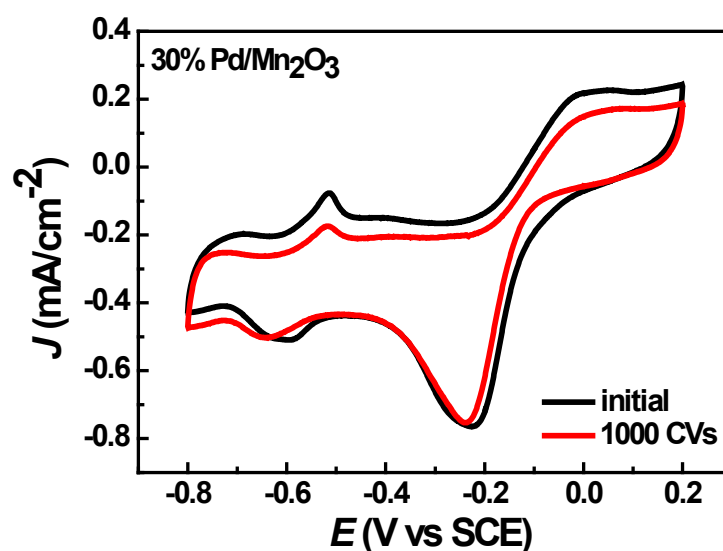


**Fig. S9** CV (50 mV/s) curves for 30% Pd-Mn<sub>2</sub>O<sub>3</sub> before and after 1000 potential cycles in O<sub>2</sub>-saturated 0.1 M KOH solution.

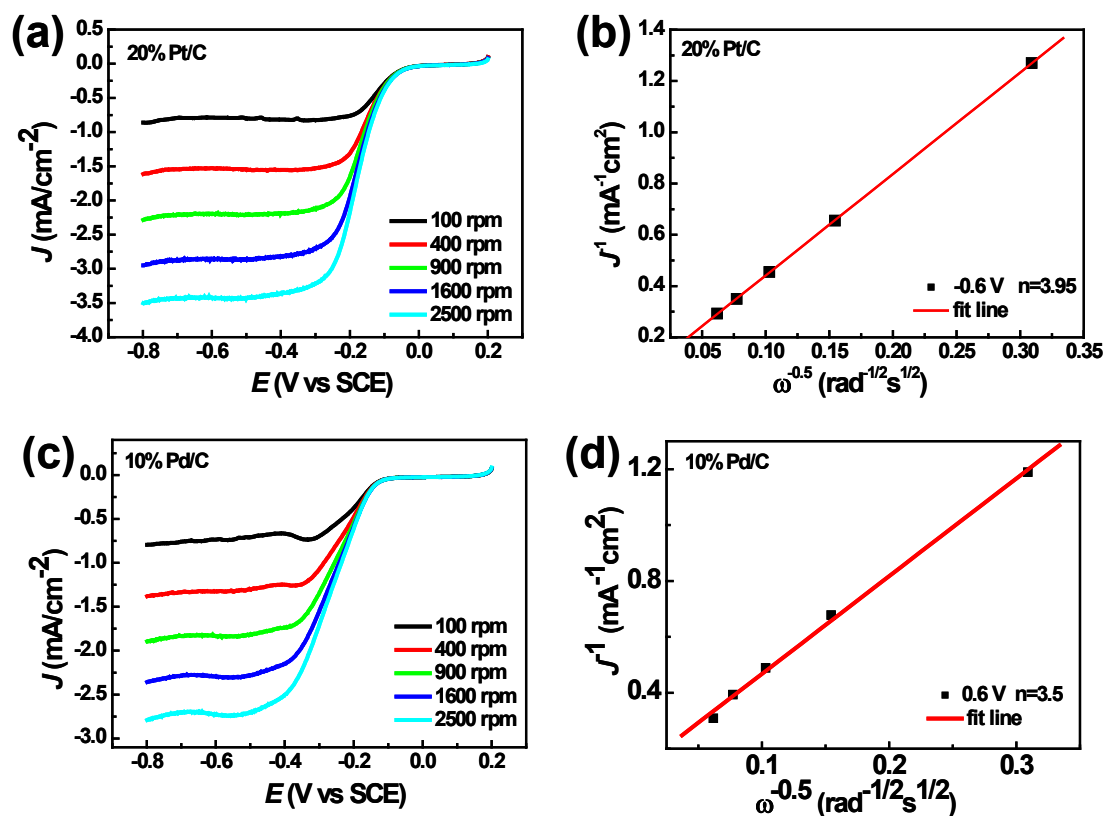


**Fig. S10** Linear scanning voltammograms for (a) 20% Pt/C and (c) 10% Pd/C and Koutecky-Levich Plots for (b) 20% Pt/C and (d) 10% Pd/C at 0.6 V.

**Table S2** Detailed results of ORR in different catalysts

catalyst	Onset potential (V vs. SCE)	Current density (mA/cm <sup>2</sup> )	Transfer number
Mn <sub>2</sub> O <sub>3</sub>	-0.15	1.89	2.4
10% Pd-Mn <sub>2</sub> O <sub>3</sub>	-0.05	2.02	3.6
20% Pd-Mn <sub>2</sub> O <sub>3</sub>	0	2.32	3.7
30% Pd-Mn <sub>2</sub> O <sub>3</sub>	0.01	2.52	4
10% Pd/C	-0.1	2.27	3.5
20% Pt/C	-0.01 (in this work) -0.03-0.03 (in previous reports)	2.85	3.9
Pd/graphene	-0.13	2.19	3.6